Available online at www.sciencedirect.com
ScienceDirect
Trans. Nonferrous Met. Soc. China 26(2016) 2363−2371
Transactions of Nonferrous Metals Society of China
www.tnmsc.cn

Extracellular green synthesis of silver nanoparticles using Amazonian fruit Araza (*Eugenia stipitata* McVaugh)

Brajesh KUMAR[1,2], Kumari SMITA[1], Alexis DEBUT[1], Luis CUMBAL[1]

1. Centro de Nanociencia y Nanotecnologia, Universidad de las Fuerzas Armadas ESPE, Av. Gral. Rumiñahui s/n, Sangolqui, P. O. Box 171-5-231B, Ecuador;
2. Department of Chemistry, TATA College, Kolhan University, Chaibasa-833202, Jharkhand, India

Received 12 August 2015; accepted 4 May 2016

Abstract: An eco-friendly method for the extracellular synthesis of silver nanoparticles (AgNPs) using aqueous Araza fruit extract and their antioxidant activity was investigated. It was observed that UV–Vis absorption peak is dependent on various parameters such as pH, temperature, and change of time. The initial appearance of the yellow color with intense surface plasmon bands at 430−450 nm, then transmission electron microscopy, scanning electron microscopy and X-ray diffraction analysis revealed the formation of 15−45 nm sized, spherical and crystalline AgNPs. Fourier transform infrared spectroscopy depicted that malic acid, citric acid, and carotenoids of Araza fruit involved in the synthesis of AgNPs. In addition, the surface modified AgNPs (77.42%, 1 mL) showed nearly double antioxidant efficiency than Araza fruit extract (35.30%, 1 mL) against 1, 1-diphenyl-2-picrylhydrazyl. The present study highlights the possibility of using the Araza fruit to synthesize AgNPs, which could be used effectively in the present and future antioxidant agent.

Key words: extracellular synthesis; silver nanoparticles; antioxidant; eco-friendliness

1 Introduction

Nowadays, extracellular biosynthesis of nano-structured materials (nanoparticles, nanorods and nanowires) using plant extracts appears to be more promising alternative than physical, chemical and microbial methods due to its simplicity, low cost, eco-friendliness and even no need to maintain an aseptic environment [1,2]. Among all metal nanoparticles, silver nanoparticles (AgNPs) have received considerable attention in recent years because of their unique properties (small size, high specific surface area) and potential applications in diverse areas, including photonics, optoelectronics, textile engineering, catalysis, water treatment, biological tagging and pharmaceutical applications [3−5]. There are numerous methods to reduce Ag^+ to AgNPs, such as sonochemical [6,7], photochemical [8], electrochemical [9], chemical/ N,N-dimethyl formamide [10], γ-rays [11], and biological techniques using fungi [12], bacteria [13], yeast [14], seed [15], root [16], fruit [17], microalga [18], leaf [19], agricultural waste [20], have been already reported.

In addition, there are scarce of scientific reports concerning the scope of Amazonian fruits for the synthesis of nanomaterials, efficiently. An important example of such a fruit is the Araza or Arazá (*Eugenia stipitata* McVaugh), which is native to the Amazon rainforest and belongs to the Myrtaceae family. It is an intense canary yellow color tropical fruit (spherical, 4−7 cm in diameter) with a delicate peel of 1 mm in thickness, which accounts for 10% of the total fruit mass and 6 to 15 seeds per fruit (Fig. 1). It has an agricultural and industrial importance due to its traditional medicinal applications, exotic tastes, juiciness, high acidity, unique sensory characteristics, and pectin content of the fruit makes it suitable to produce juice, nectars, jams, and jellies [21,22]. It contains multiple parent carotenoids as lutein, zeaxanthin, zeinoxanthin, α-carotene, β-carotene, β-cryptoxanthin, anhydrolutein, anhydrozeaxanthin, zeinoxanthin [23], malic and citric acids [22]. So, it is considered a potentially economically valuable fruit for the Andean economy.

In continuation of our ongoing research on the Andean plant materials for the synthesis of different

Corresponding author: Brajesh KUMAR; Tel: +593-2-3989492; +91-8757618562; E-mail: krmbraj@gmail.com
DOI: 10.1016/S1003-6326(16)64359-5

metal nanoparticles [20,24−26], herein we reported the use of Amozonian fruit, Araza for the extracellular synthesis, characterization and application of AgNPs (Fig. 2). We hypothesized that carotenoids, malic and citric acids of Araza fruit act as either bioreductant or stabilizer and spherical AgNPs were obtained. The as-synthesized AgNPs were characterized by UV–Vis spectroscopy, transmission electron microscopy (TEM), scanning electron microscopy (SEM), X-ray diffraction (XRD) and Fourier transform infrared (FTIR) instrumental techniques. Further, the antioxidant activity of the AgNPs was investigated by using 1, 1-diphenyl-2-picrylhydrazyl (DPPH), which will provide an important utilization of Araza fruit as new therapeutic materials.

2 Experimental

2.1 Chemicals and preparation of Araza fruit extract

All chemicals used were of analytical grade and used without any purification. Silver nitrate ($AgNO_3$, 99.0%) was purchased from Spectrum, USA, and DPPH (>99.5%) was purchased from Sigma-Aldrich, USA. Fresh unripened Araza fruit was purchased from the popular market near Universidad de las Fuerzas Armadas ESPE, Sangolqui, Ecuador. The thoroughly washed and finely chopped Araza fruit (5 g) was heated (60−62 °C) in 50 mL of Milli-Q water for 60 min. After cooling, the colorless extract was filtered using Whatman No.1 paper and stored at 4 °C for further use.

2.2 Extracellular biosynthesis of AgNPs

For the extracellular green synthesis of AgNPs, 2 mL of Araza fruit extract was mixed with 10 mL of 1 mmol/L $AgNO_3$ solution in the visible light (55−65 cd/m^2). Color changes were observed from colorless to wine red, indicating the formation of AgNPs. The effect of the pH and temperature was determined by varying the pH (4.0, 5.6, 7.0, 9.0 and 11.0) of 1 mmol/L $AgNO_3$ at temperatures of 22−25, 60−65 and 90−95 °C. The reaction mixtures were monitored at different time intervals and the synthesized AgNPs under optimized conditions were further characterized by different analytical instruments.

2.3 Evaluation of radical scavenging activity

The scavenging activity of the AgNPs was measured by using DPPH as a free radical model and a method adapted from KUMAR et al [20] with slight modifications. An aliquot (200−1000 μL) of extract/AgNPs or control, and 1000−1800 μL of H_2O was mixed with 2.0 mL of 0.2 mmol/L (DPPH) in 95% of ethanol. The mixture was vortexed vigorously and allowed to stand at room temperature (22−25 °C) for 30 min in the dark. The absorbance of the mixture was measured spectrophotometrically at 517 nm, and the free radical scavenging activity was calculated using Eq. (1):

$$y=(1-A_1/A_2)\times 100\% \quad (1)$$

where y is the scavenging percentage; A_1 is the absorbance of sample; and A_2 is the absorbance of control.

The scavenging percentages of all samples were plotted. The final result was expressed as percentage of DPPH free radical scavenging activity (mL).

Fig. 1 Unripened (a) and ripened (b) Araza fruit

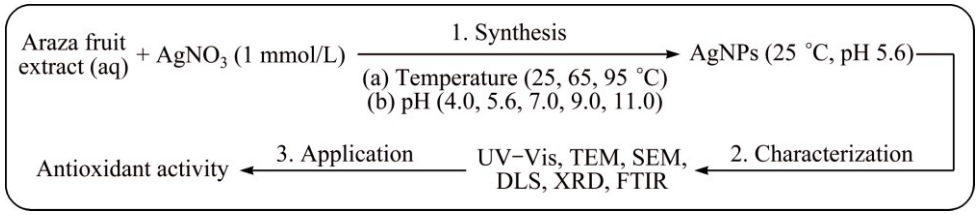

Fig. 2 Schematic stepwise flow chart for synthesis, characterization and application of AgNPs

2.4 Characterization of AgNPs

The Araza extract mediated synthesis of AgNPs was confirmed by UV−Vis spectrophotometer, Thermo Spectronic, GENESYS^{TM} 8, England. For the background correction of all the UV−Vis spectra, Milli-Q water was used. The pH measurements of $AgNO_3$ solution were done by using pH meter (Seven Easy pH, METTLER TOLEDO AG, 8603, Switzerland). The particle size distributions of nanoparticles were determined using the HORIBA, Dynamic Light Scattering (DLS) Version LB−550 program. The size, shape and selective area electron diffraction (SAED) pattern of nanoparticles were studied on TEM (FEI, TECNAI, G2 spirit twin, Holland). The surface morphology and elemental analysis of AgNPs were recorded digitally using SEM (TESCAN, MIRA 3) equipped with energy-dispersive X-ray spectrometry (EDX, Bruker Nano GmbH, Quantax). XRD studies on thin films of the nanoparticle were carried out using a PANalytical brand θ–2θ configuration (generator-detector) X-ray tube copper at λ=1.54 Å and EMPYREAN diffractometer. The functional groups on the surface of the samples were characterized by using the transmission mode (650−4000 cm^{-1}) using a Perkin Elmer spectrophotometer (FTIR Spectrum Two).

3 Results and discussion

3.1 Visual and UV−Vis study

The appearance of yellow or wine red color in a reaction mixture after addition of plant extract to $AgNO_3$ is the primary visual signature of biosynthesis of AgNPs. The optimal pH, temperature and time required for the biosynthesis of AgNPs from the extract of Araza fruit were monitored by visual and UV−Vis spectroscopy (Fig. 3). Figure 3(a) shows the visual and UV−Vis spectra of AgNPs incubated at room temperature (22−25 °C) for 18 h at different pH values. It was observed that, with increasing pH from 5.4 to 9.0, the position and intensity of absorbance peak do not increase very much. The single absorbance peak located at 430 nm yielded a characteristic single surface plasmon resonance (SPR) band of spherical and monodisperse AgNPs. MIE [27] stated that a single SPR band results in spherical nanoparticles whereas two or more SPR bands result in variation in shape. However, the increase in the basicity or acidity at pH 11.0 and 4.0 causes the absorption peaks to become broader, damped and shifted towards higher wavelengths, indicating polydispersity. The additional peak observed at 270−290 nm can be assigned to the phytochemicals of Araza fruit and their associated silver clusters, which, via intermediates, build up metallic AgNPs. For the AgNPs at pH 5.6, the color is yellowish, SPR peak is more sharp and appears to shift towards lower wavelengths (430 nm), indicating the smaller particle size [28,29].

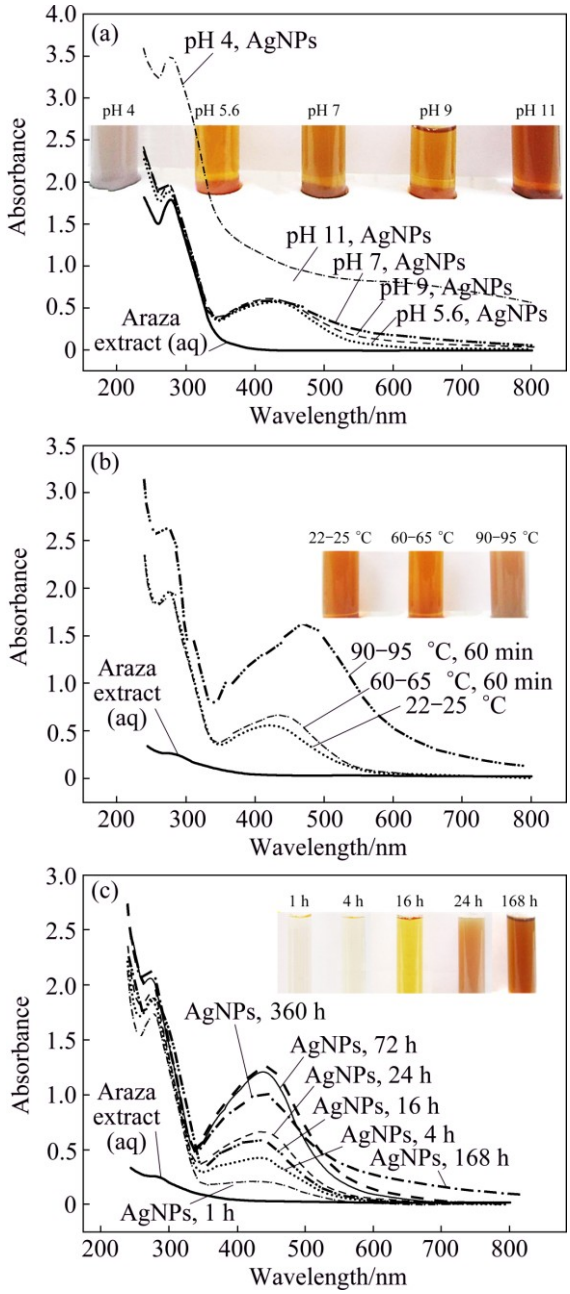

Fig. 3 Visual and UV−Vis spectra of as-synthesized AgNPs at different pH after 18 h room temperature incubation period (a), at pH 5.6 and different temperatures after 24 h room temperature incubation period (b) and at pH 5.6 and room temperature for different incubation time intervals (c)

After confirming the pH required for AgNPs synthesis, the temperature and incubation period for AgNPs synthesis were monitored. The SPR bands of AgNPs at different temperatures (22−25, 60−65 and 90−95 °C) are represented in Fig. 3(b). It showed that the AgNPs synthesized at 90−95 °C for 60 min have a maximum absorbance (1.605) at λ_{max}=470 nm signified the greater biosynthesis of bigger AgNPs, whereas the

AgNPs synthesized at 60−65 °C for 60 min and 22−25 °C have the maximum absorbance peaks at 420 and 430 nm after 24 h incubation period at room temperature. The AgNPs synthesized at 60−65 and 22−25 °C are smaller, there is no big difference in the intensity and wavelength of absorption peaks of AgNPs. So, from green synthesis point of view, room temperature (22−25 °C) and pH=5.6 are more preferred and suggested for the synthesis of AgNPs.

Finally, the reaction mixture ($AgNO_3$ and Araza fruit extract) was incubated at 22−25 °C, pH=5.6 and the absorbance was measured at different time intervals (Fig. 3(c)). It shows the visual signature for the formation of AgNPs and the color of the reaction mixture becomes darker and intensity of SPR band increases with the lapse of time. The appearance of yellow color from colorless indicates the reduction of Ag^+ to Ag and the formation of AgNPs after 4 h. UV–Vis spectrum of the reaction mixture reveals the appearance of an SPR band at 430 nm and gradually grows to be the main peak, giving the impression of red-shift (450 nm), whereas there is no significant absorption peak for the Araza fruit extract alone. The shift of wavelength from 430 to 450 nm indicates either the formation of stable aggregates of the AgNPs in solution or shape anisotropy in the particles [30]. The results of the UV−Vis spectrum (single SPR) agree with the previous report [6] that the synthesized AgNPs were found to be symmetrical, with spherical in nature. To monitor the stability of the AgNPs, the UV−Vis absorption was measured for a time period of 15 d. It was noticed that, there was no significant increase of peak intensity after 72 h to 168 h, but peak intensity was decreased after 15 d and SPR band became more broader. This may be due to the presence of oxidized phytochemicals of Araza fruit, which promotes in-situ aggregation and formation of bigger AgNPs.

3.2 TEM−SAED study

TEM images and SAED patterns of as-prepared AgNPs after 24 h are elucidated in Fig. 4. It is evident that the as-prepared AgNPs are spherical and well dispersed, and the average size is in the range of 15−45 nm (Figs. 4(a)–(d)). The measurement of the size was performed along the largest diameter of the particles. Little bit agglomerates are also present due to the accumulation of small nanosized crystals (Fig. 4(e)). The SAED pattern of AgNPs (Fig. 4(f)) is recorded from the spherical Ag nanostructures and it clearly shows the circular fringes corresponding to the ring like electron diffraction patterns, typical of polycrystalline AgNPs. The diffraction rings of the AgNPs have been indexed as (111), (200) and (220), which are consistent with the face centered cubic (FCC) structure of Ag [15].

3.3 SEM−EDX study

Chemical characterization in the SEM was performed non-destructively with EDX analysis. SEM images, including EDX mapping of AgNPs are shown in Fig. 5. It clearly shows the homogeneous distribution of

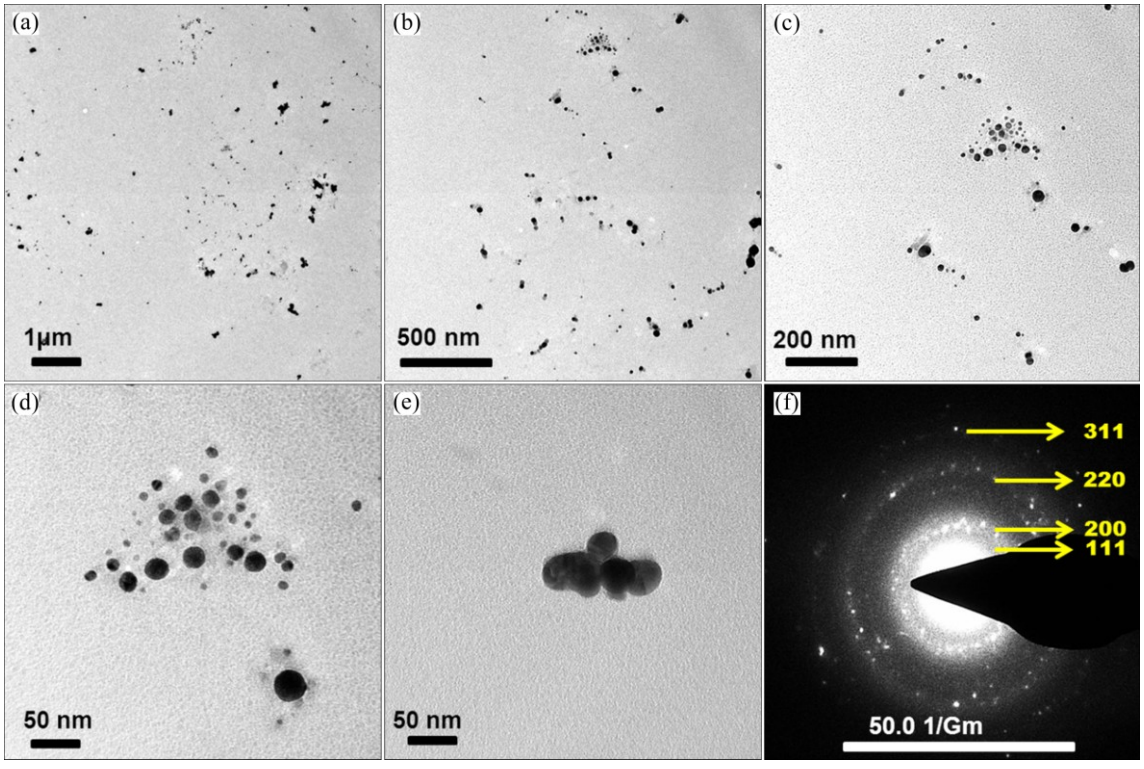

Fig. 4 TEM (a−e) and SAED (f) images of synthesized AgNPs

AgNPs in a large area (Fig. 5(a)). To better observe the distribution of AgNPs, the corresponding EDX/elemental mapping analysis was carried out. Figures 5(b) and (c) show the homogeneous distribution of large amounts of elemental carbon and oxygen. From Fig. 5(d), we can infer the presence of well dispersed metallic silver in the form of AgNPs. The EDX analysis is shown in Fig. 6 and Table 1, which clearly shows a spectral signal in the silver region at ~3.0 keV, supporting the formation of AgNPs [31]. Peaks of carbon, oxygen and other elements (Na, K, Mg, Si, S, etc.) were also obtained due to the presence of phytochemicals associated metal salts in Araza fruit extract.

3.4 DLS study

The DLS analysis was used to find out the hydrodynamic size of nanoparticles. Figure 7 clearly indicates that the average particle size distribution of AgNPs is (52.8±24.8) nm and it is slightly deviated from the results of TEM images. This is due to the screening of small particles by bigger ones and attachment of Araza phytochemicals on the surface of AgNPs [32].

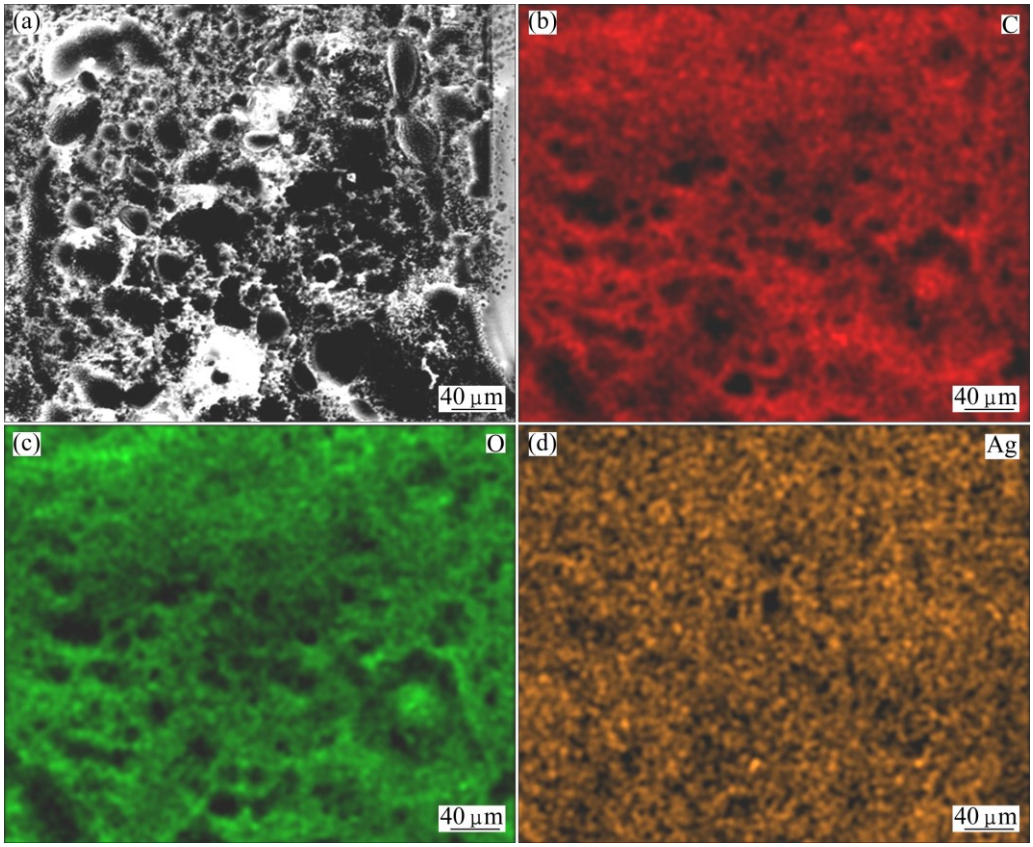

Fig. 5 SEM image of AgNPs (a) and corresponding elemental mapping images of C (b), O (c) and Ag (d)

Table 1 Elemental composition of AgNPs synthesized using Araza fruit extract

Element	AN	Series	Net	Mass fraction/%	Mole fraction/%	Error in mass fraction/% (1 Sigma)
Carbon	6	K-series	127577	39.21743	47.94388	4.385934
Oxygen	8	K-series	158477	54.35452	49.88445	6.006603
Sodium	11	K-series	5716	0.593774	0.379245	0.066757
Magnesium	12	K-series	4113	0.25529	0.154231	0.040723
Aluminium	13	K-series	2055	0.092964	0.050592	0.030458
Silicon	14	K-series	20938	0.564895	0.295338	0.05025
Phosphorus	15	K-series	6492	0.216799	0.102777	0.034316
Sulfur	16	K-series	8151	0.251069	0.114969	0.034836
Potassium	19	K-series	57286	2.011889	0.755578	0.086965
Silver	47	L-series	28755	1.364254	0.18571	0.068866
Tin	50	L-series	19360	1.077108	0.133231	0.058026

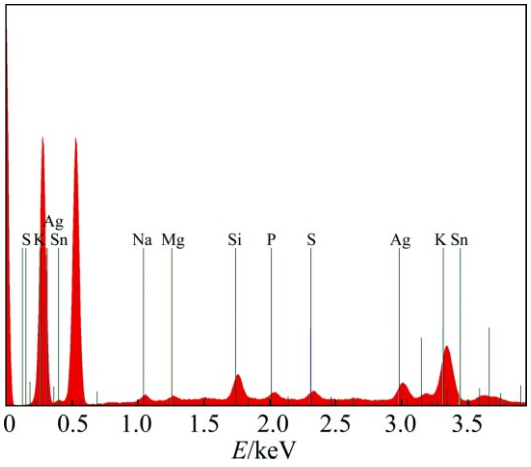

Fig. 6 EDS spectrum of AgNPs synthesized using Araza fruit extract

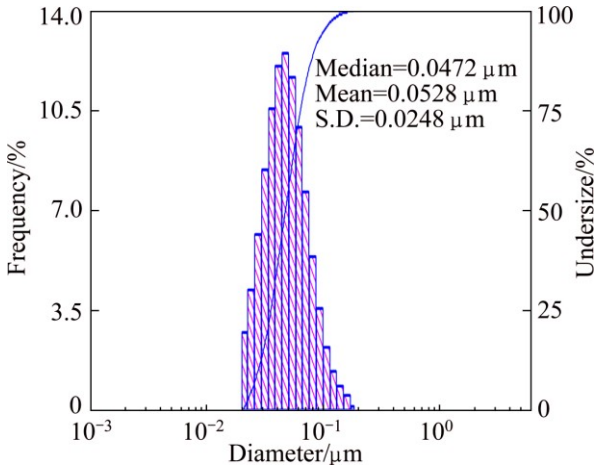

Fig. 7 Histogram of particle size distribution of AgNPs synthesized using Araza extract

3.5 XRD study

The XRD pattern of as-prepared AgNPs is shown in Fig. 8. Four intense peaks were observed at 38.11°, 44.34°, 64.48° and 77.49° (ICSD No. 98−004−4387) due to the corresponding (111), (200), (220) and (311) reflection planes of the FCC structure of silver, respectively [33,34]. The XRD analysis confirmed that AgNPs formed by the reduction of Ag^+ ions are crystalline in nature. The most intense peak corresponding to the predominant orientation of Ag nanocrystals is along (111) plane and Debye–Scherrer equation predicts that the average AgNPs size is less than 50 nm.

3.6 FTIR study

Table 2 and Fig. 9 show the FTIR spectra of dried Araza fruit extract and as-synthesized AgNPs. The strong, broadband, appearing at 3285 cm^{-1} in the FTIR spectrum in Fig. 9(a) can be associated with stretching vibrations

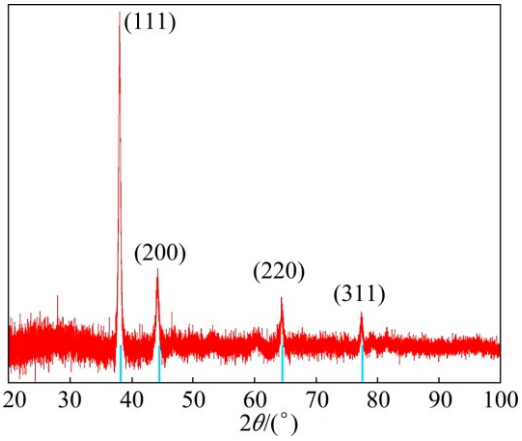

Fig. 8 XRD pattern of synthesized AgNPs

Table 2 Different FTIR peaks of Araza fruit extract/AgNPs and their significant functional groups

No.	Wavenumber of Araza fruit extract/cm^{-1}	Functional group	Wavenumber of AgNPs/cm^{-1}	Functional group
1	3285	Stretching vibrations of O—H bonds	3306	—OH stretching, Ag—OH
2	2919	Asymmetrical and symmetrical stretching vibrations of —CH_2— bonds	–	–
3	1715	Stretching vibration of C═O of —COOH	–	–
4	1630	Stretching vibration of C═O of —CONH/amide I	1637	C═O stretching, C═O—Ag
5	1588	Stretching vibrations of C═C aliphatic	–	–
6	1402	Bending vibration of —OH		
7	1226	Stretching vibration of C—O ester groups and bending vibration of —CH_2— group	–	–
8	1097, 1030	Stretching vibration of C—O group in alcohol and carboxylic acid	–	–
9	889	Bending vibrations of trans-disubstituted C—H	–	–

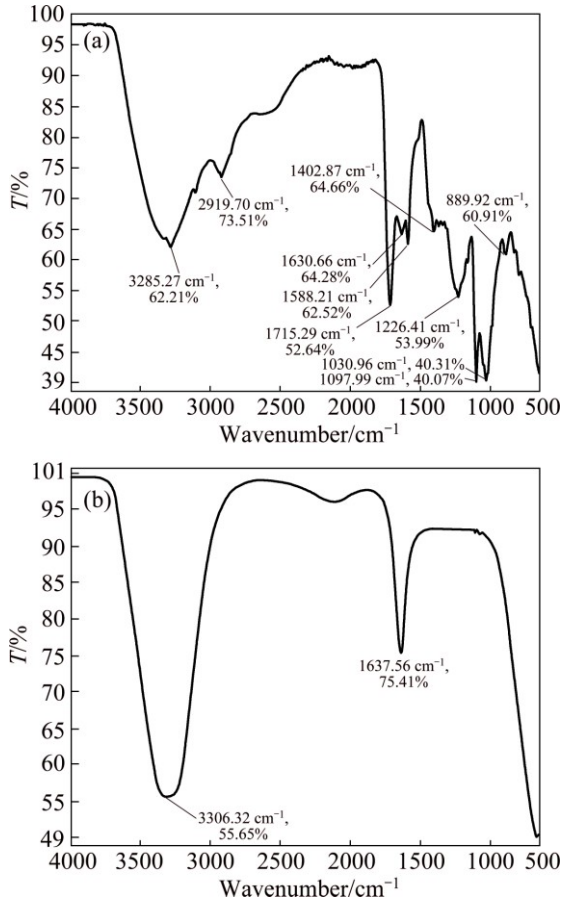

Fig. 9 FTIR spectra of Araza extract (a) and synthesized AgNPs (b)

of O−H bonds, in alcohols and phenols (cellulose, pectin, etc.), whereas the peak at 2919 cm^{-1} corresponds to the stretching vibration of the —CH_2— compound [20].

The bands at around 1715 and 1630 cm^{-1} correspond to the C═O stretching vibration of —COOH and amide I [23]. Peaks observed at around 1588, 1402 and 1226 cm^{-1} correspond to C═C aliphatic, O—H bending and C—O stretching vibration, whereas 1097 and 1030 cm^{-1} correspond to C—O stretching from alcohol and carboxylic acid, respectively. In addition, the weak peak at 889 cm^{-1} is characteristics of trans-disubstituted C—H bending of alkenes [35]. After bioreduction (Fig. 9(b)), there is a shift of the absorption band of 3285 to 3306 cm^{-1} and 1630 to 1637 cm^{-1}, indicating the involvement of —OH and C═O in the formation of AgNPs. It also confirms the AgNPs capped with the water soluble extract containing —COOH and —OH groups.

3.7 Mechanism of reduction of Ag^+ to AgNPs

The major phytochemicals present in the Araza fruit are malic acid, citric acid and carotenoids (lutein, zeaxanthin, zeinoxanthin, α-carotene, β-carotene, β-cryptoxanthin, anhydrolutein, anhydrozeaxanthin, zeinoxanthin) [22,23]. The possible mechanism for the reduction of Ag^+ is proposed and presented in Fig. 10. In this scheme, Ag^+ ions can interact with O—H groups, which subsequently undergo oxidation to —CHO and —COOH forms with consequent reduction of Ag^+ to AgNPs. Finally, — COOH groups help in the stabilization of AgNPs.

3.8 Evaluation of antioxidant activity

The excessive production of free radicals (·OH, ·NO, ·OR, etc.) in cells during oxidative stress, metabolism and respiration lead to many pathological disorders like aging, heart attack, and cancer. Antioxidants are the chemical moiety which transfers an electron to the free radicals and prevents the generation of oxidant stress by making stable paired electrons [36]. One of the quickest methods to evaluate the antioxidant activity is the scavenging activity on DPPH. DPPH is a stable free radical which can accept hydrogen or electron from donors and gets reduced by a color change from purple to yellow. The antioxidant activity of both Araza fruit extract and AgNPs were estimated against DPPH with different dosages (mL), as shown in Fig. 11. It was observed that, scavenging activity (%) of both samples increases with the increase of the dose-dependent concentration and found to be maximum of 77.42% for

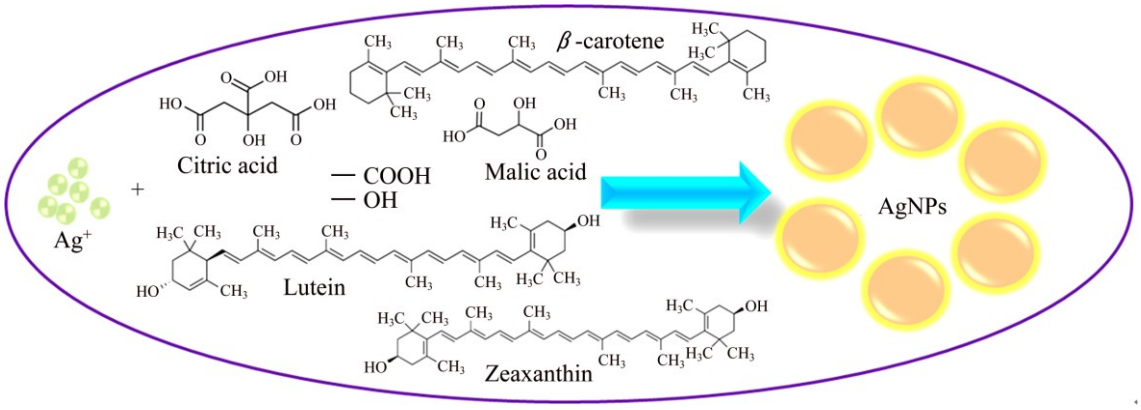

Fig. 10 Suggested schematic diagram for biosynthesis of AgNPs using fruit extract of Araza

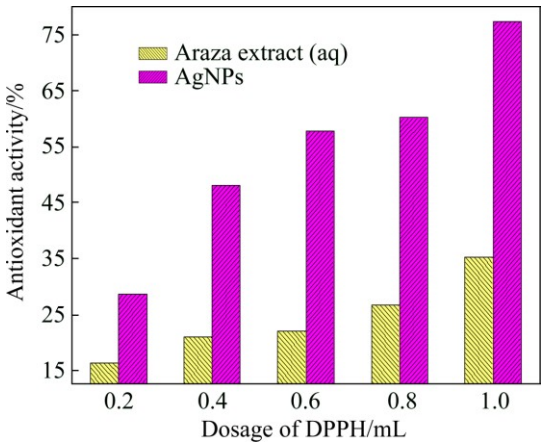

Fig. 11 Antioxidant activity of Araza extract and synthesized AgNPs against dosage of DPPH

AgNPs and 35.30% for Araza fruit extract in 1 mL. The dramatic increase of antioxidant efficacy of AgNPs might be the synergistic result of an active physicochemical interaction of Ag atoms with the functional groups (COO^-, O^-) of the Araza fruit extract and high surface area of the spherical AgNPs [20,26,33].

4 Conclusions

This study demonstrated that the Araza fruit extract has the potential to be used as reducing and stabilizing agents for the extracellular synthesis of AgNPs in an eco-friendly protocol. Various characterization techniques such as UV−Vis, TEM, SEM, DLS, XRD and FTIR confirmed that Ag^+ was reduced to AgNPs. It was found that the synthesized AgNPs were spherical, 15−45 nm sized, crystalline and SPR band around 430−450 nm. This eco-friendly surface modified AgNPs exhibited higher antioxidant efficacy than Araza fruit extract and can potentially be used in biomedical applications.

Acknowledgments

This scientific work has been funded by the Prometeo Project of the National Secretariat of Higher Education, Science, Technology and Innovation (SENESCYT), Ecuador.

References

[1] RAVEENDRAN P, FU J, WALLEN S L. Completely "green" synthesis and stabilization of metal nanoparticles [J]. Journal of American Chemical Society, 2003, 125: 13940−13941.

[2] RAI A, SINGH A, AHMAD A, SASTRY M. Role of halide ions and temperature on the morphology of biologically synthesized gold nanotriangles [J]. Langmuir, 2006, 22: 736−741.

[3] KELLY K L, CORONADO E, ZHAO L L, SCHATZ G C. The optical properties of metal nanoparticles: The influence of size, shape and dielectric environment [J]. The Journal of Physical Chemistry B, 2003, 107: 668−677.

[4] JAVAD HOSSEINI S, AGHAIE H, GHAEDI M. The synthesis of Ag nanoparticles and loading it on activated carbon as a novel adsorbent for removing methyl orange by using surface response methodology [J]. Oriental Journal of Chemistry, 2014, 30: 1883−1895.

[5] RAVANANA M, GHAEDI M, ANSARI A, TAGHIZADEH F, ELHAMIFAR D. Comparison of the efficiency of Cu and silver nanoparticle loaded on supports for the removal of Eosin Y from aqueous solution: Kinetic and isotherm study [J]. Spectrochimica Acta Part A: Molecular and Biomolecular Spectroscopy, 2014, 123: 467−472.

[6] KUMAR B, SMITA K, CUMBAL L, DEBUT A, PATHAK R N. Sonochemical synthesis of silver nanoparticles using starch: A comparison [J]. Bioinorganic Chemistry and Applications, 2014, 2014: 784268.

[7] JAMSHIDI M, GHAEDI M, DASHTIAN K, HAJATI S, BAZRAFSHAN A. Ultrasound-assisted removal of Al^{3+} ions and Alizarin red S by activated carbon engrafted with Ag nanoparticles: Central composite design and genetic algorithm optimization [J]. RSC Advances, 2015, 5: 59522−59532.

[8] CALLEGARI A, TONTI D, CHERGUI M. Photochemically grown silver nanoparticles with wavelength-controlled size and shape [J]. Nano Letters, 2003, 3: 1565−1568.

[9] YIN B, MA H, WANG S, CHEN S. Electrochemical synthesis of silver nanoparticles under protection of poly(N-vinylpyrrolidone) [J]. The Journal of Physical Chemistry B, 2003, 107: 8898−8904.

[10] PASTORIZA-SANTOS I, LIZ-MARZÁN L M. Formation and stabilization of silver nanoparticles through reduction by N, N-dimethyl formamide [J]. Langmuir, 1999, 15: 948−951.

[11] WANG S, ZHANG Y, MA H L, ZHANG Q, XU W, PENG J, LI J, YU Z Z, ZHAI M. Ionic-liquid-assisted facile synthesis of silver nanoparticle-reduced graphene oxide hybrids by gamma irradiation [J]. Carbon, 2013, 55: 245−252.

[12] NAYAK R R, PRADHAN N, BEHERA D, PRADHAN K M, MISHRA S, SUKLA L B, MISHRA B K. Green synthesis of silver nanoparticle by *Penicillium purpurogenum* NPMF: The process and optimization [J]. Journal of Nanoparticle Research, 2011, 13: 3129−3137.

[13] GOPINATHAN P, ASHOK A M, SELVAKUMAR R. Bacterial flagella as biotemplate for the synthesis of silver nanoparticle impregnated bionanomaterial [J]. Applied Surface Science, 2013, 276: 717−722.

[14] MISHRA A, TRIPATHY S K, YUN S I. Bio-synthesis of gold and silver nanoparticles from *Candida guilliermondii* and their antimicrobial effect against pathogenic bacteria [J]. Journal of Nanoscience and Nanotechnology, 2011, 11: 243−248.

[15] DHAND V, SOUMYA L, BHARADWAJ S, CHAKRA S, BHATT D, SREEDHAR B. Green synthesis of silver nanoparticles using *Coffea arabica* seed extract and its antibacterial activity [J]. Materials Science and Engineering C, 2016, 58: 36−43.

[16] SHAMELI K, AHMAD M B, ZAMANIAN A, SANGPOUR P, SHABANZADEH P, ABDOLLAHI Y, ZARGAR M. Green biosynthesis of silver nanoparticles using *Curcuma longa* tuber powder [J]. International Journal of Nanomedicine, 2012, 7: 5603−5610.

[17] KUMAR B, SMITA K, CUMBAL L, DEBUT A, CAMACHO J, HERNÁNDEZ-GALLEGOS E, CHÁVEZ-LÓPEZ M G, GRIJALVA M, ANGULO Y, ROSERO G Y A, GUSTAVO R. Pomosynthesis and biological activity of silver nanoparticles using *Passiflora tripartita* fruit extracts [J]. Advanced Materials Letters, 2015, 6(2): 127−132.

[18] JENA J, PRADHAN N, NAYAK R R, DASH B P, SUKLA L B, PANDA P K, MISHRA B K. Microalga *Scenedesmus* sp.: A potential low-cost green machine for silver nanoparticle synthesis [J]. Journal

of Microbiology and Biotechnology, 2014, 24(4): 522−533.

[19] GHAEDIA M, YOUSEFINEJAD M, SAFARPOOR M, ZARE KHAFRI H, PURKAIT M K. *Rosmarinus officinalis* leaf extract mediated green synthesis of silver nanoparticles and investigation of its antimicrobial properties [J]. Journal of Industrial and Engineering Chemistry, 2015, 31: 167−172.

[20] KUMAR B, SMITA K, CUMBAL L, ANGULO Y. Fabrication of silver nanoplates using *Nephelium lappaceum* (Rambutan) peel: A sustainable approach [J]. Journal of Molecular Liquids, 2015, 211: 476−480.

[21] LIZCANO L J, BAKKALI F, RUIZ-LARREA M B, RUIZ-SANZ J I. Antioxidant activity and polyphenol content of aqueous extracts from *Colombian Amazonian* plants with medicinal use [J]. Food Chemistry, 2010, 119: 1566−1570.

[22] HERNÁNDEZ M S, MARTÍNEZ O, FERNÁNDEZ-TRUJILLO J P. Behavior of arazá (*Eugenia stipitata* Mc Vaug) fruit quality traits during growth, development and ripening [J]. Scientia Horticulturae, 2007, 111: 220−227.

[23] GARZÓN G A, NARVÁEZ-CUENCA C E, KOPEC R E, BARRY A M, RIEDL K M, SCHWARTZ S J. Determination of carotenoids, total phenolic content, and antioxidant activity of Arazá (*Eugenia stipitata* McVaugh), an Amazonian fruit [J]. Journal of Agricultural and Food Chemistry, 2012, 60: 4709−4717.

[24] KUMAR B, SMITA K, CUMBAL K, CAMACHO J, HERNÁNDEZ-GALLEGOS E, CHÁVEZ-LÓPEZ M G, GRIJALVA M, ANDRADE K. One pot phytosynthesis of gold nanoparticles using *Genipa americana* fruit extract and its biological applications [J]. Materials Science and Engineering C, 2016, 62: 725−731.

[25] KUMAR B, SMITA K, CUMBAL L, DEBUT A. Biogenic synthesis of iron oxide nanoparticles for 2-arylbenzimidazoles fabrication [J]. Journal of Saudi Chemical Society, 2014, 18: 364−369.

[26] KUMAR B, SMITA K, CUMBAL L, DEBUT A. Ultrasound agitated phytofabrication of palladium nanoparticles using Andean blackberry leaf and its photocatalytic activity [J]. Journal of Saudi Chemical Society, 2015, 19(5): 574−580.

[27] MIE G. Contribution to the optical properties of turbid media, in particular of colloidal suspensions of metals [J]. Annals of Physics (Leipzig), 1908, 25: 377−452.

[28] NIDYA M, UMADEVI M, SANKAR P, RAJKUMAR B J M. L-Glutamic acid functionalized silver nanoparticles and its nonlinear optical applications [J]. Journal of Materials Science: Materials in Electronics, 2015, 26(6): 4124−4131.

[29] NAYAK D, ASHE S, RAUTA P R, KUMARI M, NAYAK B. Bark extract mediated green synthesis of silver nanoparticles: Evaluation of antimicrobial activity and antiproliferative response against osteosarcoma [J]. Materials Science and Engineering C, 2016, 58: 44−52.

[30] JIN R, CAO Y W, MIRKIN C A, KELLY K L, SCHATZ G C, ZHENG J G. Photoinduced conversion of silver nanospheres to nanoprisms [J]. Science, 2001, 294: 1901−1903.

[31] KUMAR V, SINGH D K, MOHAN S, HASAN S H. Photo-induced biosynthesis of silver nanoparticles using aqueous extract of *Erigeron bonariensis* and its catalytic activity against Acridine Orange [J]. Journal of Photochemistry and Photobiology B: Biology, 2016, 155: 39−50.

[32] KHLEBTSOV B N, KHLEBTSOV N G. On the measurement of gold nanoparticle sizes by the dynamic light scattering method [J]. Colloid Journal, 2011, 73(1): 118−127.

[33] SREEKANTH T V M, RAVIKUMAR S, EOM I Y. Green synthesized silver nanoparticles using *Nelumbo nucifera* root extract for efficient protein binding, antioxidant and cytotoxicity activities [J]. Journal of Photochemistry and Photobiology B: Biology, 2014, 141:100−105.

[34] MEHMOOD A, MURTAZA G, BHATTI TM, RAFFI M, KAUSAR R. antibacterial efficacy of silver nanoparticles synthesized by a green method using bark extract of *Melia azedarach* L [J]. Journal of Pharmaceutical Innovation, 2014, 9: 238−245.

[35] RAO K J, PARIA S. Green synthesis of silver nanoparticles from aqueous *Aegle marmelos* leaf extract [J]. Materials Research Bulletin, 2013, 48(2): 628−634.

[36] RAJAN A, VILAS V, PHILIP D. Catalytic and antioxidant properties of biogenic silver nanoparticles synthesized using *Areca catechu* nut [J]. Journal of Molecular Liquids, 2015, 207: 231−236.

用亚马逊地区水果提取物(*Eugenia stipitata* McVaugh)细胞体外绿色合成银纳米颗粒

Brajesh KUMAR[1,2], Kumari SMITA[1], Alexis DEBUT[1], Luis CUMBAL[1]

1. Centro de Nanociencia y Nanotecnologia, Universidad de las Fuerzas Armadas ESPE, Av. Gral. Rumiñahui s/n, Sangolqui, P. O. Box 171-5-231B, Ecuador;

2. Department of Chemistry, TATA College, Kolhan University, Chaibasa-833202, Jharkhand, India

摘　要：提出一种用亚马逊地区水果提取物(液态)细胞体外合成银纳米颗粒(AgNPs)的生态友好方法，并研究其抗氧化活性。结果表明：AgNPs 的紫外−可见光吸收峰与各参数如 pH 值、温度和时间相关。初始黄色样品在波长为 430~450 nm 范围的强吸收峰、透射电镜、扫描电镜及 X 射线衍射分析结果表明，形成了尺寸为 15~45 nm、球状 AgNPs 晶体。傅里叶变换红外光谱表明 AgNPs 的合成与苹果酸、柠檬酸和类胡萝卜素有关。此外，经表面改性的 AgNPs(77.42%，1 mL)对 2,2−二苯基−1−苦肼基的抗氧化效率是 Araza 果实提取物的(35.30%，1 mL)的 2 倍。此研究为采用 Araza 果实提取物合成 AgNPs 提供了可行性，所合成的 AgNPs 可用作有效的抗氧化剂。

关键词：细胞体外合成；银纳米颗粒；抗氧化剂；生态友好

(Edited by Wei-ping CHEN)